

## APPLICABILITY OF THE HIGH VELOCITY COMBUSTION WIRE (HVCW) SPRAYING PROCESS FOR THE DEPOSITION OF PROTECTIVE METALLIC COATINGS

### Marcos F. O. Schiefler Fo.

Federal Center for Technological Education – CEFET-PR  
Av. Sete de Setembro 3165, 80230-901, Curitiba-PR, Brazil  
schiefler@cefetpr.br

### Augusto J. A. Buschinelli

Federal University of Santa Catarina – UFSC  
Mailbox 476, 88040-900, Florianópolis-SC, Brazil  
buschi@emc.ufsc.br

### Frank Gärtner

Helmut-Schmidt University of the Federal Armed Forces  
Holstenhofweg 85, 22043, Hamburg, Germany  
frank.gaertner@hsu-hh.de

### Heinrich Kreye

Helmut-Schmidt University of the Federal Armed Forces  
Holstenhofweg 85, 22043, Hamburg, Germany  
heinrich.kreye@hsu-hh.de

**Abstract.** *Thermally sprayed metallic coatings used for protection against corrosion are very suitable for both, on- and offshore applications. This is possible not only because they provide cathodic and/or barrier-type protection to the substrate, but also due to the ease by which they can be applied onto large surfaces. However, conventional spray techniques such as Flame (FS) and Arc Spraying (AS), which are still widely used in the industry, supply coatings showing a very peculiar morphology. Those coatings normally contain many defects in the microstructure (e.g., pores, oxides and cracks), whose amount and distribution can severely restrain their service life and performance. In order to minimize that deficiency, the more recently introduced High Velocity Combustion Wire (HVCW) spraying process appears as an alternative for high-quality coatings, which are produced at relatively low costs. It operates with higher particle velocities, resulting in lower porosity and finer coating microstructures as compared to conventional techniques. The goal of this paper is to verify the efficiency of the HVCW process concerning the protection of steel components and structures against atmospheric marine corrosion. For that purpose, a wide microstructural and corrosion behaviour characterization was carried out on different anodic Al- and cathodic Fe-Cr-(Ni)-based coatings. According to the obtained results, the advantages of the HVCW process depend on the nobleness of the spray material and, in addition, the influence of microstructural characteristics on the mechanical and tribological properties of the coatings could be satisfactorily determined. Moreover, the ability of the use of electrochemical techniques to rank the different coatings could be proved.*

**Keywords:** *thermal spraying, HVCW process, metallic coatings, corrosion protection, electrochemical techniques.*

### 1. Introduction

Aiming to protect low carbon and low-alloyed steel components against atmospheric marine corrosion and wear, the deposition of metallic coatings with suitable properties becomes ever more a good alternative. Basically, there are two types of coatings that could be applied for that purpose. The first method involves a physical barrier-type corrosion resistant coating (i.e., paint or a more noble metal alloys) between the steel substrate and the corrosive environment. The second one involves an active (less noble) metal coating, which protects the steel substrate by its sacrificial behavior as anode. Among the commercial techniques, Thermal Spraying (TS) is considered as one of the most versatile to apply both types of the above-mentioned protective metallic coatings.

Thermal spraying is a manufacturing process in which a metal, polymer or ceramic metal in the form of a powder, wire or rod is continuously fed into a gun, which heats the material to near or above its melting temperature. At the same time, a gas stream accelerates the molten, semi-molten or solid particles that are formed and directs them onto a substrate surface, on which a coating is formed (Pawlowski, 1995). A major advantage of thermal spraying is the wide variety of materials that can be used. It should be stressed, however, that the microstructure of thermally sprayed coatings, which results from the solidification and sintering of the sprayed particles, frequently contain defects like pores, oxides and cracks. These features result in material properties less desirable than those obtained from bulk materials produced through melting and deformation. The amount and distribution of the defects, as well as other

coating properties as for instance hardness and bond strength, will be defined by the selected spray parameters. Therefore, the correct choice of the spray process as well as respective parameters (i.e., fuel gas type, particle velocity, spray distance and so on) is very important for the deposition of efficient coatings and, consequently, to enlarge the useful life in service of the coated parts and structures.

Concerning coating materials, typical anodic coatings for corrosion protection of the steel are based on aluminum, zinc or their alloys (Fitzsimons, 1996 and Totlani *et al.*, 2000). On the other hand, more noble coatings as stainless steels or Ni-based alloys, which exhibit a cathodic behavior compared to the substrate, can have serious limitations for that function, because any defect may allow the electrolyte to reach the coating/substrate interface. In that situation, severe under-corrosion will take place at the underlayer metal, due to the large cathode/anode area ratio that is created. Despite these limitations, the use of corrosion resistant alloy coatings has aroused much interest over the recent years (Hofman *et al.*, 1998; Eminoglu *et al.*, 1999; Kuroda *et al.*, 2000; Sturgeon, 2001; Zhang *et al.*, 2002 and Schiefler *et al.*, 2004). This fact could be explained by the continuous development of better spray systems, which are ever more able to produce coatings of higher quality.

## 2. The High Velocity Combustion Wire (HVCW) Spraying Process

The introduction of the so-called High Velocity Oxy-Fuel Flame (HVOF) spraying process, twenty-five years ago, improved the quality of coatings sprayed by conventional procedures, like for example Flame (FS) or Arc Spraying (AS) processes (Irving *et al.*, 1993). This technique has as special features a smaller heating of the coating materials and remarkably higher impact velocities on the surfaces which are to be coated (Kreye *et al.*, 2000). Thus, it is possible to produce denser coatings which are more securely bonded to the substrate, as well as other favorable properties. On the other hand, a disadvantage of the HVOF process is regarding its significantly higher application costs, mainly because of the feedstock material as powder and due to the higher oxy-fuel consumption.

The more recently developed High Velocity Combustion Wire (HVCW) spraying process can be a possibility of obtaining coatings showing at the same time high quality and low costs. Its guns are in fact smaller HVOF systems, which have been designed particularly for wires, and differ from the conventional wire spraying systems (Flame and Arc) with respect to their significantly higher operating pressures. In addition, these systems use a stream of compressed air, which serves for cooling as well as for accelerating the flame stream (Kreye *et al.*, 2001).

The HVCW system illustrated in Fig. 1a operates at 4.0 bars propane, 8.0 bars oxygen and 7.0 bars of compressed air, as opposed to 3.0 bars propane, 3.0 bars oxygen and 4.5 bars of compressed air for the case of conventional Flame Spraying. Consequently, a finer atomization of the molten wire tip and higher particle velocities are obtained, resulting in more refined microstructures. By using wires with a diameter of 3.2 mm, typical spraying rates of 2.0 kg/h for aluminum and Hastelloy C-276, 8.0 kg/h for steel and 4 kg/h for molybdenum are achieved (Kreye *et al.*, 2000), which are similar to those of HVOF process. For steel as feedstock material, the deposition efficiency can be so high as 80%.

Figure 1b proposes a model for the atomization process at the wire tip, whereas Fig. 2 shows a real image of the plume, which is formed after a HVCW gun nozzle. In the former illustration, the droplets are produced because of the presence of wave instabilities in the liquid metal. In the latter illustration, a series of shock diamonds is visible in the plume, due to the supersonic velocity of the gas stream leaving the nozzle (see also the atomization process in Fig. 1b). The image showed in Fig. 2 was obtained by means of a high-speed digital camera.

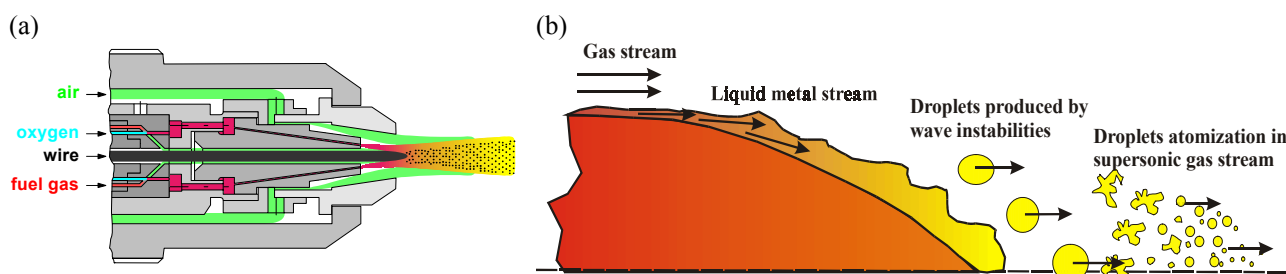


Figure 1. (a) HVw 2000 system for High Velocity Combustion Wire (HVCW) spraying process. (b) Schematic illustration showing the formation of droplets during the atomization process at the wire tip.

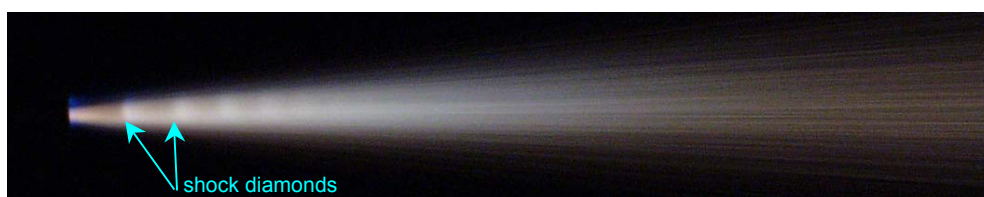


Figure 2. Real image of the plume containing shock diamonds formed after a HVCW gun nozzle. Spraying of Hastelloy C-276 with propane as fuel gas and wire feed rate of 1.6 m/min (HVw 2000 system).

For comparison, Fig. 3 shows typical microstructures of AlMg5 coatings which were sprayed by conventional Flame and Arc Spraying, as well as by High Velocity Combustion Wire spraying (Schiefler *et al.*, 2003). The micrographs clearly demonstrate the higher density of the HVCW coatings. These coatings are superior, also because they normally show a higher bond strength and a smoother surface.

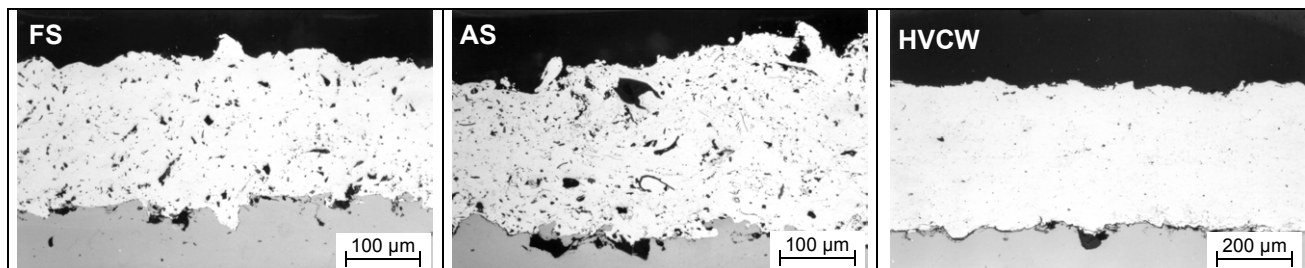


Figure 3. Typical cross-section microstructures of AlMg5 coatings sprayed by different processes (OM images).

The aim of the following study was to verify the efficiency of the HVCW process for spraying different protective metallic coatings. For that purpose, a microstructural and electrochemical characterization was carried out on various coatings based on aluminum or zinc (Al99.5, AlMg5, ZnAl15 and Al99.5+W<sub>2</sub>C), iron-chromium (DIN X46Cr 13 and AISI 316L stainless steels) and nickel (Hastelloy C-276). Coating microstructures were examined before and after electrochemical testing (corrosion potential monitoring and polarization resistance tests), in order to investigate the influence of defects like pores, oxides and cracks on the corrosion performance.

### 3. Materials and Methods

#### 3.1. Production of Coatings

All coatings were sprayed on degreased and freshly grit-blasted DIN St 37 (1.0037  $\approx$  ASTM S235) low carbon steel substrates, nominally 50x70x4 mm<sup>3</sup> in size. The grit blasting process was carried out with corundum particles of 0.1-1.0 mm in diameter. HVCW spraying was performed either with the W 1000 system from Metatherm GmbH, Homburg, Germany, or the HVw 2000 system from High Velocity Technologies Inc., West Lebanon, NH, USA. Its operation principles were already schematically presented in Fig. 1. Commercially available wires of 1.60 or 3.16 mm in diameter were used as feedstock material, except for Al99.5+W<sub>2</sub>C coatings, which were sprayed using a filled wire of 1.70 in diameter. The commercial spray systems and parameters related to the different coatings are summarized in Table 1.

Table 1. Thermal spray systems and respective spray parameters used for the different HVCW coatings.

Parameter / Coating Material	Al99.5	AlMg5	ZnAl15	Al99.5+W <sub>2</sub> C	X46Cr13	316L	Hast. C-276
Spray System	W 1000	HVw 2000	W 1000	HVw 2000	W 1000	W 1000	HVw 2000
Wire Diameter (mm)	3.16	1.60	3.16	1.70	1.60	3.16	1.60
Wire Feed Rate (m/min)	1.03	4.80	1.04	4.80	0.60	0.43	1.60
Spray Distance (mm)	215	250	325	250	150	215	180
Number of Passages	4	6	5	4	14	10	12
Fuel Gas (bar / l/min)	Propane 3.5 /	Ethylene 3.9 / 34	Propane 3.8 /	Ethylene 3.9 / 34	Propane 3.4 / 35	Propane 3.5 /	Propane 3.7 / 23
Oxygen (bar / l/min)	5.0 /	4.0 / 94	2.4 /	4 / 93	2.1 / 55	7.0 /	4.1 / 92
Compressed Air (bar / l/min)	6.5 /	5.9 / 506	6.0 /	5.9 / 507	5.0 / 464	6.5 /	5.8 / 542
Cooling	Air/CO <sub>2</sub>	---	---	---	---	Air/CO <sub>2</sub>	---

#### 3.2. Coating Characterization

##### 3.2.1. Metallographic Preparation and Microscopic Analysis

Metallographic samples were prepared from coated specimens. Basically, the experimental procedure was composed of the following steps: (a) application of a protective resin on the surface to be analyzed; (b) cross sectioning using abrasive wheel by a Struers equipment model Discotom-2; (c) embedding of the samples in cold mounting resin; (d) automatic grinding with abrasive papers (grits 320, 500 and 1000), according to specific routines developed for Struers equipment model RotoPol-31; (e) automatic polishing of the samples by the same equipment, using diamond suspensions with grain sizes of 6, 3, 1 and 0.25 µm. In some cases, OPS solution from Struers was also utilized. After preparation, the different morphologies were analyzed by optical microscopy using a Leica microscope model DM.

### 3.2.2. Microstructural and Mechanical Properties Characterization

The measurements of thickness were carried out on polished cross sections by using optical microscopy (OM). The images were displayed on a video monitor and the values were taken from a digital measurement system. The oxygen content of the coatings was determined by the inert gas fusion technique, using a Leco TC-436-DR equipment. The coating porosity was determined by quantitative image analysis on the basis of optical micrographs taken from cross sections at magnifications of 100X or 500X, depending on the thickness of the specimen. The surface roughness was measured by a digital equipment from Taylor Hobson, model Surtronic 3+, according to standard DIN 4768.

Microhardness tests were conducted in accordance to the standard DIN 50133, using a Vickers diamond pyramid indenter from Leitz. The measurements were performed with loads of 0.98 (100 gf) or 2.94 N (300 gf), depending of the coating type, on polished cross sections of the specimens. The bond strength of coatings was tested according to standard DIN EN 582, in which cylinders of 25 mm diameter were coated on one side, glued to a grit blasted counter body and pulled apart in a tensile testing machine. Finally, the wear tests were performed in accordance to the Japanese standard JIS H 8615. As output value, the mass loss after 1200 double strokes was taken.

### 3.2.3. Electrochemical Characterization

The corrosion behavior of the coatings was valued by means of corrosion potential monitoring ( $E_{\text{corr}}$  vs.  $t$ ) and polarization resistance ( $R_p$ ) tests. All experiments were set up in freshly prepared 1 mol/l NaCl solution as electrolyte, after cleaning the specimens with purified water, degreasing them with ethanol in an ultrasonic bath and final drying under hot air stream. For anodic coatings, both  $E_{\text{corr}}$  vs.  $t$  and  $R_p$  procedures were successively carried out for a total duration of 960 hours, whereas the cathodic coatings were tested within 96 hours immersion. The latter ones were investigated in three different conditions: as-sprayed, as-sprayed + detached from the substrate and as-sprayed + sealing. An epoxy resin sealant from GTV GmbH (Luckenbach, Germany) type D 350 was employed to seal them. For comparison purposes,  $E_{\text{corr}}$  vs.  $t$  tests were also performed on bulk St 37 and bulk material (X46Cr 13 wire, 316L and Hastelloy C-276 sheets). In both cases, the specimens were grinded up to grit size 1000 and properly cleaned.

The electrochemical cells used in the  $E_{\text{corr}}$  vs.  $t$  and  $R_p$  tests consisted of conventional two- and three-electrode arrangements, respectively. The coated specimen was the working electrode (WE) and a standard Calomel electrode (SCE) served as reference (RE), whereas a platinum wire mesh was used as counter electrode (CE). For  $E_{\text{corr}}$  vs.  $t$  experiments, the assembled cells were filled with the electrolyte and closed inside a Faraday shield, where the temperature was controlled to a set point of  $30 \pm 1^\circ\text{C}$ . During the first 96 hours of test, potential and temperature values were automatically stored on a computer with a sampling rate of 1/60 Hz. After this time the data were averaged over 48 hours, until reaching the total duration of 960 hours. The exposed area of the specimens was  $1 \text{ cm}^2$  and the experiment configuration allowed simultaneous testing of three cells.  $R_p$  measurements were conducted at room temperature with commercial potentiostat and software (273a model and 352 SoftCorr III version, respectively, both from EG&G, Princeton, USA). In that case, the coated specimens were potentiodynamically polarized to a range of  $-25 \text{ mV} \leq E_{\text{corr}} \leq +25 \text{ mV}$  at a rate of  $0.167 \text{ mV/s}$ , while measuring the corrosion current ( $I_{\text{corr}}$ ) with respect to the CE.

## 4. Results and Discussion

Results from image analyses and key parameters like oxygen content, coating roughness and hardness are summarized in Table 2. Typical microstructures of the investigated anodic coatings as obtained from cross sections are shown in Fig. 4. The micrographs allow comparing the coatings in the as-sprayed condition and after immersion for 960 hours ( $E_{\text{corr}}$  vs.  $t$  +  $R_p$  tests). Close-ups from the latter are also included. It can be noted that there is a good correspondence between the measured values (Table 2) and the characteristics of the microstructures in Fig. 4. For all coatings based on aluminum, it can be also observed that the initial corrosive attack remains concentrate on the surface regions, which occurs probably due to their relatively lower oxygen content, porosity and surface roughness.

Table 2. Microstructural characteristics and properties determined for various HVCW anodic and cathodic coatings.

Property / Coating Material	Thickness ( $\mu\text{m}$ )	O <sub>2</sub> Content (wt.%)	Porosity (vol.%) <sup>(1)</sup>	Roughness, $R_a$ ( $\mu\text{m}$ )	Micro-hardness <sup>(2)</sup>	Bond Strength (MPa) <sup>(1)</sup>	Mass Loss (mg/1200DS) <sup>(1)</sup>
Al99.5	610 $\pm$ 10	0,34 $\pm$ 0,01	2,0	10,4 $\pm$ 0,6	40 $\pm$ 5	25,9	---
AlMg5	545 $\pm$ 65	0,36 $\pm$ 0,03	4,0	12,8 $\pm$ 0,6	86 $\pm$ 6	8,1	---
ZnAl15	560 $\pm$ 20	0,21 $\pm$ 0,01	7,0	9,0 $\pm$ 0,3	34 $\pm$ 2	23,7	---
Al99.5+W <sub>2</sub> C	285 $\pm$ 05	0,50 $\pm$ 0,03	4,0	12,0 $\pm$ 0,3	65 $\pm$ 4	15,0	49,1
X46Cr13 steel	245 $\pm$ 20	8,55 $\pm$ 0,28	2,0	13,4 $\pm$ 1,3	570 $\pm$ 39	76,9	91,0
316L steel	285 $\pm$ 25	6,97 $\pm$ 0,07	0,7	9,3 $\pm$ 1,2	353 $\pm$ 43	42,7	112,0
Hastelloy C-276	315 $\pm$ 40	1,77 $\pm$ 0,02	0,1	8,3 $\pm$ 1,5	282 $\pm$ 20	55,8	127,10

<sup>(1)</sup>: mean values. <sup>(2)</sup>: HV0.1 for Al99.5, AlMg5 and ZnAl15 coatings; HV0.3 for the remaining ones; in the case of Al99.5+W<sub>2</sub>C coatings, the measurements were made directly on the matrix phase.

Previous work (Schiefler *et al.*, 2003) has shown that the mechanisms by which the corrosion process occurs for corresponding FS and AS coatings are quite different. In those cases, the bigger amount of defects in the microstructure facilitates the permeability of the electrolyte across the sprayed particles.

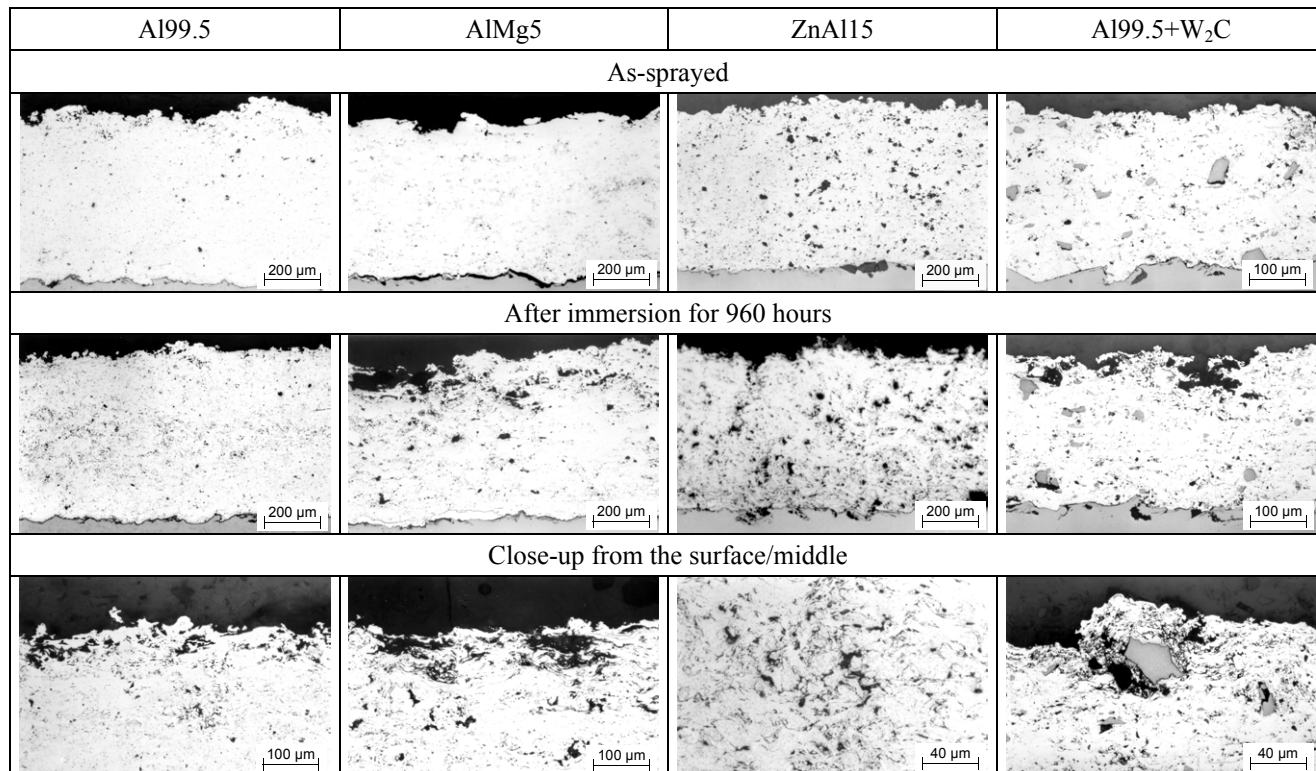


Figure 4. Cross-section microstructures of investigated HVCW anodic coatings (OM images).

The potential monitoring ( $E_{\text{corr}}$  vs.  $t$ ) for long duration testing of 960 hours is summarized for various HVCW anodic coatings in Fig. 5a. Corresponding results from  $R_p$  investigations are presented in Fig. 5b. Figure 5a is showing that the open circuit potentials ( $E_{\text{corr}}$ ) for times of up to 960 hours range approximately between -1030 to -800 mV.  $E_{\text{corr}}$  of the low carbon steel was determined after stabilization as about -730 mV vs. SCE (Schiefler *et al.*, 2002). As expected, this  $E_{\text{corr}}$  is nobler than those of the anodic coatings. Higher is the difference between the corrosion potentials of coatings and substrate, the more effective is the sacrificial protection by the coating material.

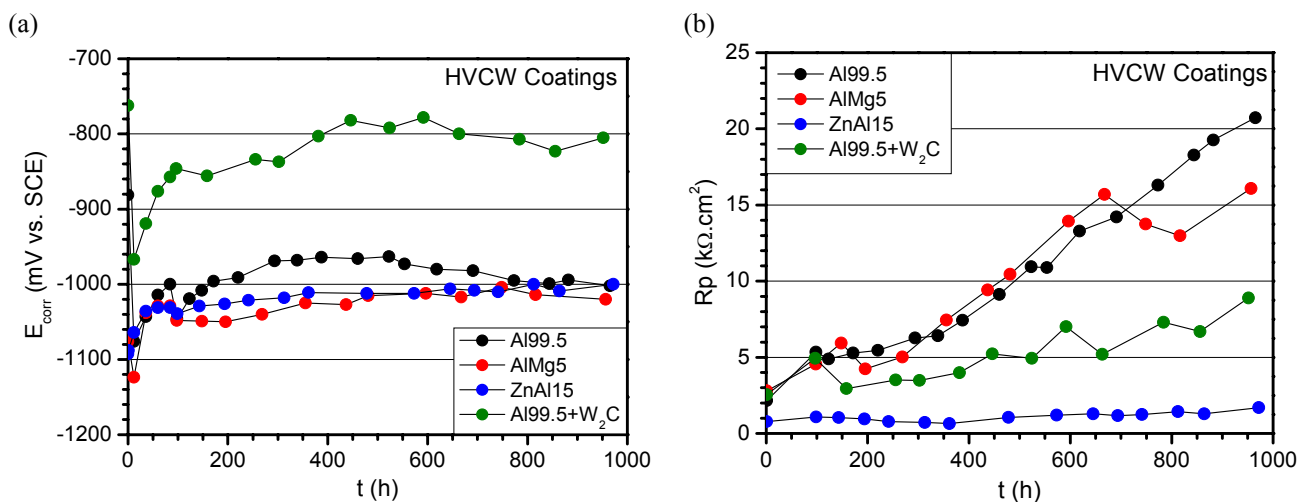


Figure 5. (a) Comparison among potential measurements for various HVCW anodic coatings within 960 hours immersion; (b) Corresponding polarization resistance measurements.

The most negative potential after testing was obtained for the AlMg5 coating (about -1030 mV). As expected,  $E_{\text{corr}}$  values of AlMg5 and ZnAl15 coatings became more negative along the experiment than  $E_{\text{corr}}$  value of Al99.5. In theory,



this can be explained because both magnesium and zinc were electrochemically less noble than aluminum. It can be also noted that, except for Al99.5+W<sub>2</sub>C, the corrosion potentials tend to the same value after testing. Due to the presence of tungsten carbides in the microstructure,  $E_{\text{corr}}$  of the Al99.5+W<sub>2</sub>C coating became clearly more positive in comparison to potential values developed from the others anodic coatings. Based on the  $E_{\text{corr}}$  curves in Fig. 5a, it can be observed that the coatings reach their steady states at different immersion times, but it could be considered that after about 100 hours, all coatings have more or less reached their respective potential stabilization.

Figure 5b shows that the  $R_p$  evolutions are different for the coatings during the immersion period. Initially, the corrosion rates are relatively high and the formed corrosion products are gradually blocking pores and cracks in the coating microstructures. Consequently, the first  $R_p$  values measured after 1 hour are relatively low and under  $4 \text{ k}\Omega\cdot\text{cm}^2$  for all investigated anodic coatings. Following that initial phase, the substrate is effectively isolated from the electrolyte, and the time necessary to reach this situation depends on the coating characteristics. Figure 5a revealed that after about 100 hours immersion, the  $E_{\text{corr}}$  values remain approximately constant.  $R_p$  values in Fig. 5b are still increasing, however, mainly for Al99.5 and AlMg5 coatings beyond this time. A possible explanation for this behavior is the continued development of a passivating oxide film, which additionally limits the electrode reaction rate on the surface of the coating (Vreijling *et al.*, 1998). The presence of nobler W dissolved in the Al matrix may cause the formation of small galvanic corrosion sites, which would contribute to prevent any process of passivation on the surface of the Al99.5+W<sub>2</sub>C coating. Actually, the corresponding  $R_p$  values showed in Fig. 5b remain relatively low and constant along the test. Concerning ZnAl15 coating, the constant very low  $R_p$  values result from its inability to passivate. Zn is more active in comparison to Al and its corrosion products are not so adherent to the coating surface (Schiefler *et al.*, 2005). Because of that, they are highly soluble in NaCl-based solutions and, thus, can be easily dissolved.

Typical microstructures of the investigated cathodic coatings as obtained from cross sections are shown in Fig. 6. The micrographies allow comparing the coatings in the as-sprayed condition and after immersion for 96 hours ( $E_{\text{corr}}$  vs.  $t$  tests). Close-ups from the latter are also presented for a better understanding. The two last micrographies are showing corrosive attack of the substrate at its interface with the more noble coating. Apparently, such attack has not occurred for X46Cr 13 coating. This fact indicates that the investigated HVCW 316L and Hastelloy C-276 coatings were not dense enough, in order to avoid that the electrolyte reached the substrate. Despite the different coating materials, the different oxygen contents, whose measured values are presented in Table 2, have directly reflected on the relative amount of oxides (gray phase) formed in the microstructures. Finally, it can be stressed that there is a good correspondence between the measured values (Table 2) and the characteristics of the microstructures in Fig. 6.

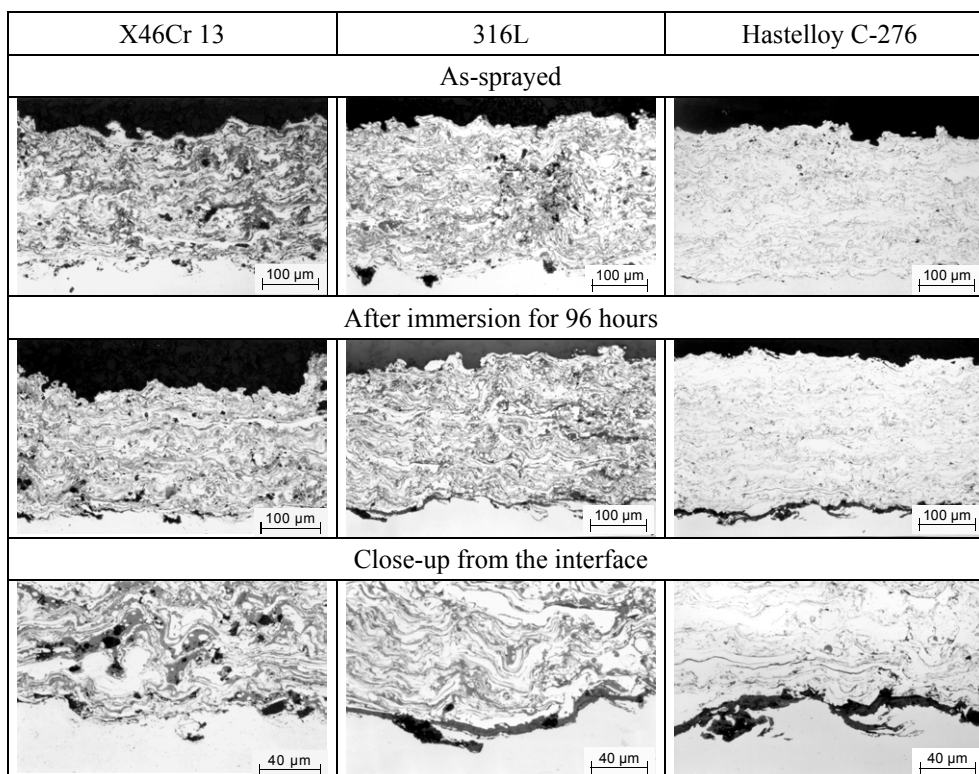


Figure 6. Cross-section microstructures of investigated HVCW cathodic coatings (OM images).

The potential monitoring curves within 96 hours immersion for X46Cr 13, 316L and Hastelloy C-276 coatings are shown in Fig. 7 (a, b and c plots, respectively). For comparison purposes, the plots include also the potential development for respective bulk material, detached and sealed coatings, as well as for substrate material (St 37 steel).

Once eliminated the direct contact with the substrate, all detached coatings have presented  $E_{\text{corr}}$  values more positives and, consequently, closer to the corrosion potential of the respective bulk materials. Therefore, it can be assumed that the potentials measured for X46Cr 13, 316L and Hastelloy C-276 as-sprayed coatings are, in really, mixed potentials derived from coating and substrate. This fact confirms that the electrolyte really reaches the substrates, permeating through the defects present in the coating microstructures, as already illustrated in the corresponding microographies in Fig. 6. This difference in behavior is more pronounced for the Hastelloy C-276 coating (Fig. 7c). Curiously,  $E_{\text{corr}}$  values for both detached and sealed X46Cr 13 coatings became more positive compared to the  $E_{\text{corr}}$  for bulk material (Fig. 7a).

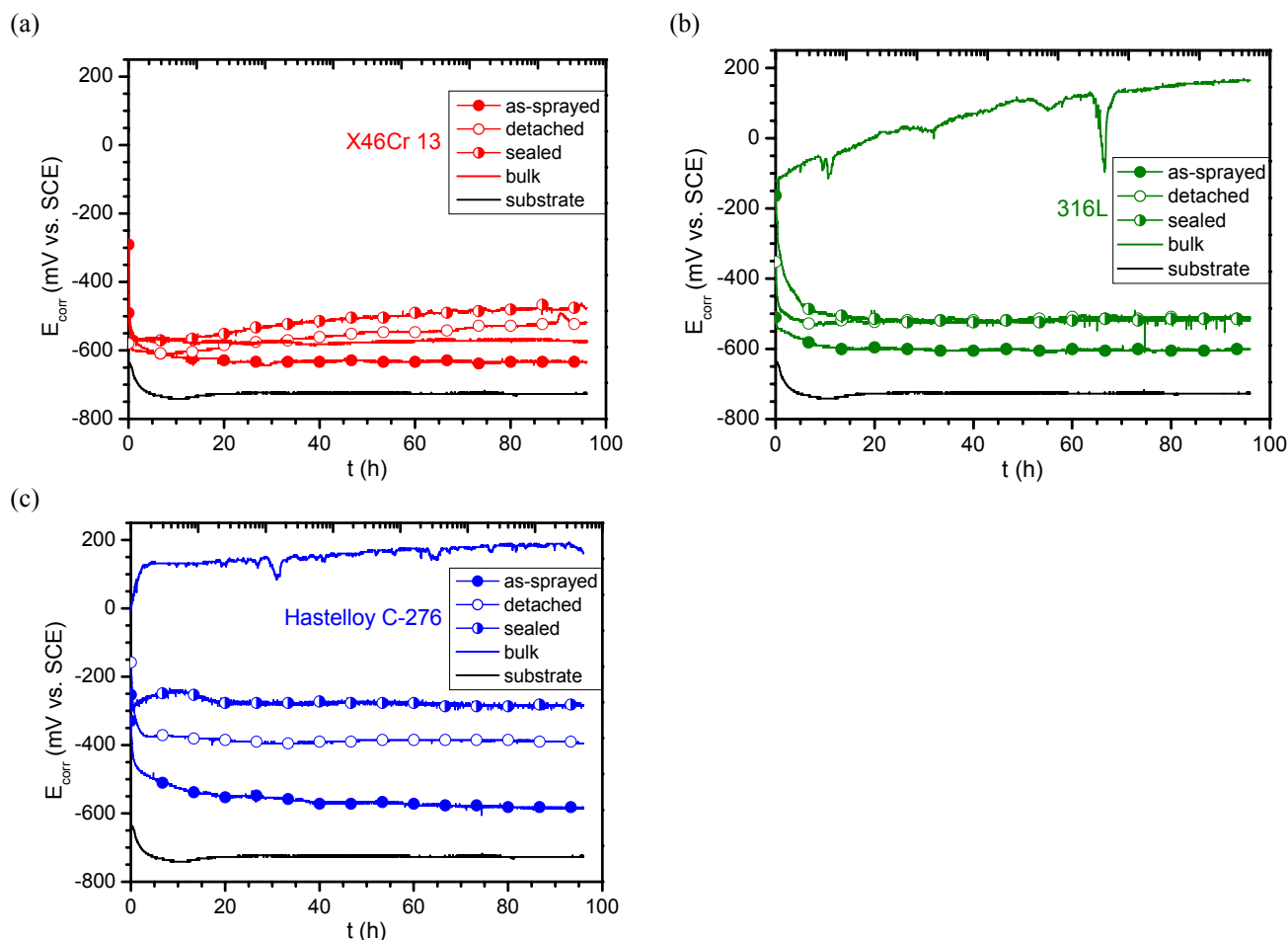


Figure 7. Comparison among potential measurements for HVCW X46Cr 13 (a), 316L (b) and Hastelloy C-276 (c) coatings within 96 hours immersion. The plots also include the potential development for respective bulk materials, detached and sealed coatings, as well as for substrate material (St 37 steel).

## 5. Summary and Conclusions

It was possible to confirm that by using high velocity spray systems like HVCW, finer microstructures with less interconnecting pores or cracks are obtained. The smoother surface indicates that the HVCW spray process is producing finer particles from the tip of the melting wire. Particularly for cathodic coatings, the results reveal that by using this process remarkable high bond strength are obtainable. Such coatings offer, in theory, better corrosion resistance than coatings applied by conventional Flame or Arc Spraying. According to the obtained results, the advantages of the HVCW process depend on the nobleness of the spray material. In addition, the influence of microstructural characteristics on the mechanical and tribological properties of the coatings could be satisfactorily determined.

The comparison of various anodic coatings on Al- and Zn-basis, which were processed by HVCW systems, reveals significant differences with respect to their performance concerning corrosion protection. Except for ZnAl15, it could be also shown that the initial corrosive attack remains concentrate on the surface region of the coatings. This occurs probably due to the relatively lower oxygen content, lower porosity and lower surface roughness supplied by the HVCW spray process, as commented above. With respect to low  $E_{\text{corr}}$  and high  $R_p$ , Al99.5 and AlMg5 coatings showed best performance after 960 hours immersion. In some applications, the more positive potential presented by Al99.5+W<sub>2</sub>C coating could be compensated for a substantial better performance regarding wear performance.

Despite of the use of HVCW spray process, electrochemical investigations carried out on X46Cr 13, 316L and Hastelloy C-276 showed that the efficiency of as-sprayed cathodic coatings for corrosion protection is still limited. In

most cases, therefore, their applications would require an additional sealant to minimize the inherent amount of microstructural defects. In the present investigations,  $E_{\text{corr}}$  values of the cathodic coatings in the detached and sealed conditions became always more positive along the time, which signify absence of direct contact between electrolyte and substrate. Furthermore, all as-sprayed cathodic coatings showed less noble corrosion potentials in comparison to the ones of respective bulk materials, which can be attributed to compositional changes due to the spraying process. The potential differences were significantly larger for 316L and Hastelloy C-276.

Moreover, the electrochemical techniques used in these investigations supplied consistent results and therefore proved their reliability to assess different corrosion behaviors.

## 6. Acknowledgements

The authors would like to express their thanks to the CAPES/Brazil and DAAD/Germany foundations for the scholarship of Mr. Schiefler.

## 7. References

- Eminoglu, C.M., Knight, R., DeFalco, J. and Dorfman, M., 1999, "Potentiodynamic Corrosion Testing of HVOF Sprayed Stainless Steel Alloy", Proceed. of the UTSC 99, Düsseldorf, Germany, pp. 39-44.
- Fitzsimons, B., 1996, "Thermal Sprayed Metal Coatings for Corrosion Protection", Protective Coatings Europe (PCE), March 1996, pp. 24-32.
- Hofman, R., Vreijling, M.P.W., Ferrari, G.M. and De Wit, J.H.W., 1998, "Electrochemical Methods for Characterisation of Thermal Spray Corrosion Resistant Stainless Steel Coatings", Materials Science Forum, Vols. 289-292, pp. 641-654.
- Irving, B., Knight, R., Smith, R.W., 1993, "The HVOF Process – The Hottest Topic in the Thermal Spray Industry", Welding Journal, AWS, V. 72, No. 7, pp. 25-30.
- Kreye, H., Gärtner, F., Kirsten, A. and Schwetzke, R., 2000, "High Velocity Oxy-Fuel Flame Spraying – State of the Art, Prospects and Alternatives", 5<sup>th</sup> HVOF Colloquium, D. Böhme, P. Heinrich, M. Petersson, H. Kreye (Eds.), GTS e. V., Unterschleißheim, Germany, pp. 5-18 (published in English and German).
- Kreye, H., Kirsten, A., Gärtner, F., Qi, X. and Krömmel, W., 2001, "High Velocity Combustion Wire Spraying - Systems and Coatings", ITSC 2001, C. C. Berndt, K. A. Khor and E. F. Lugscheider (Eds.), ASM International, Materials Park, Ohio, USA, pp. 461-466.
- Kuroda, S., Fukushima, T., Kodama, T. and Sasaki, M., 2000, "Microstructure and Corrosion Resistance of HVOF Sprayed 316L Stainless Steel and Ni Base Alloy Coatings", Proceed. of the 1<sup>st</sup> International Thermal Spray Conference, Montréal, Canada, pp. 455-462.
- Pawlowski, L., 1995, "The Science and Engineering of Thermal Spray Coatings", John Wiley & Sons Ltd, UK, 414 p.
- Schiefler Fo., M.F.O., Voyer, J., Gärtner, F. and Qi, X., 2002, "Corrosion Behaviour of High Velocity Combustion Wire Sprayed Coatings", ITSC 2002, E. Lugscheider, C. C. Berndt (Eds.), DVS – German Welding Society, Düsseldorf, Germany, pp. 553-558.
- Schiefler Fo., M.F.O., Gärtner, F., Voyer, J., Kirsten, A., Kreye, H., Buschinelli, A.J.A., 2003, "Protection of Steel Components against Marine Corrosion by Thermally Sprayed Anodic Coatings", ITSC 2003, B. R. Marple, C. Moreau (Eds.), ASM International, Ohio, USA, 10p.
- Schiefler Fo., M.F.O., Buschinelli, A.J.A., Gärtner, F., Kirsten, A., Voyer, J., Kreye, H., 2004, "Influence of Process Parameters on the Quality of Thermally Sprayed X46Cr13 Stainless Steel Coatings", J. Braz. Soc. Mech. Sci. & Eng., Jan./Mar. 2004, V. 26, No. 1, pp. 98-106, ISSN 1678-5878.
- Schiefler Fo., M.F.O., Gärtner, F., Kreye, H., Buschinelli, A.J.A., 2005, "Investigation of the Corrosion Mechanisms of Thermally Sprayed ZnAl15 Coatings", 25<sup>th</sup> Brazilian Congress of Corrosion, Salvador-BA, Brazil, Paper No. 043, 13p – (published in Portuguese, CD ROM).
- Sturgeon, A.J., 2001, "Microstructure Characteristics and Corrosion Behaviour of HVOF Sprayed Metallic Coatings", Proceed. of the Int. Thermal Spray Conference (ITSC 2001), Singapore, pp. 1149-1155.
- Totlani, M. K., Grover, A. K., Athavale, S. N., Papachan, A. L., 2000, "Corrosion Protection by Metallic Coatings", Transactions of the Metal Finishers' Association of India, V. 9, No. 4, pp. 227-237.
- Vreijling, M.P.W., Hofman, R., Van Westing, E.P.M., Ferrari, G.M. and De Wit, J.H.W., 1998, "The Use of Electrochemical Measurement Techniques towards Quality Control and Optimisation of Corrosion Properties of Thermal Spray Coatings", Materials Science Forum, Vols. 289-292, pp. 595-606.
- Zhang, D. Harris, S.J., McCartney, D.G., 2002, "An Investigation of the Corrosion Behaviour of Ni- and Co-based Alloys Sprayed with Gas and Liquid Fuel HVOF Guns", Proceed. of the International Thermal Spray Conference (ITSC 2002), Essen, Germany, pp. 500-505.

## 8. Responsibility notice

The authors are the only responsible for the printed material included in this paper.